

Electronic Supplementary Information

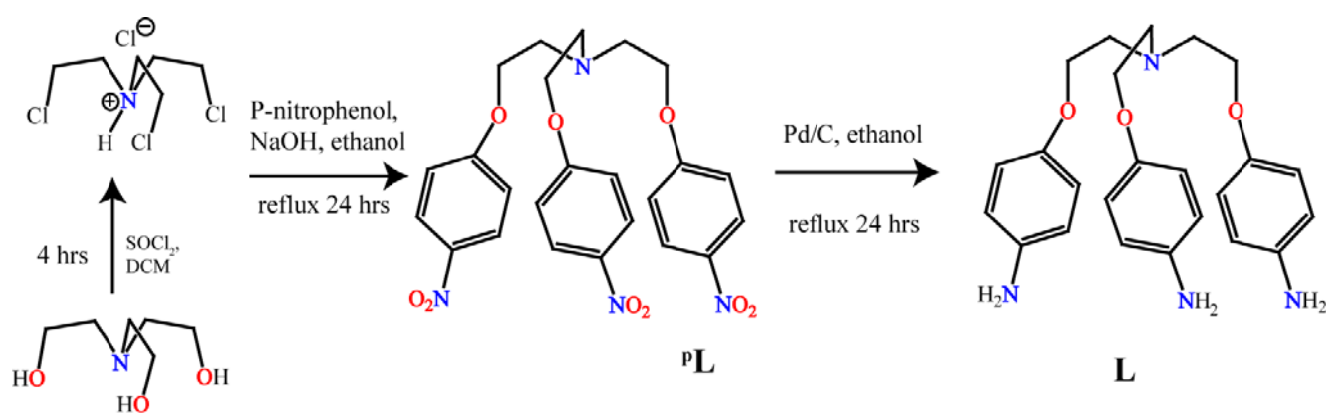
**Hydrated anion glued capsular and non-capsular assembly of a tripodal host: solid state
recognition of bromide-water $[Br_5-(H_2O)_6]^{5-}$ and iodide-water $[I_2-(H_2O)_4]^{2-}$ clusters in
cationic tripodal receptor**

Md. Najbul Hoque^a and Gopal Das*^a

Department of Chemistry, Indian Institute of Technology Guwahati, Assam, 781 039, India.

Fax: +91-361-258-2349; Tel: +91-361-258-2313

E-mail: gdas@iitg.ernet.in



Scheme 1. Preparation of Tris[2-(4-nitrophenoxy)ethyl]amine (^p**L**) and Tris[2-(4-aminophenoxy)ethyl]amine (**L**)

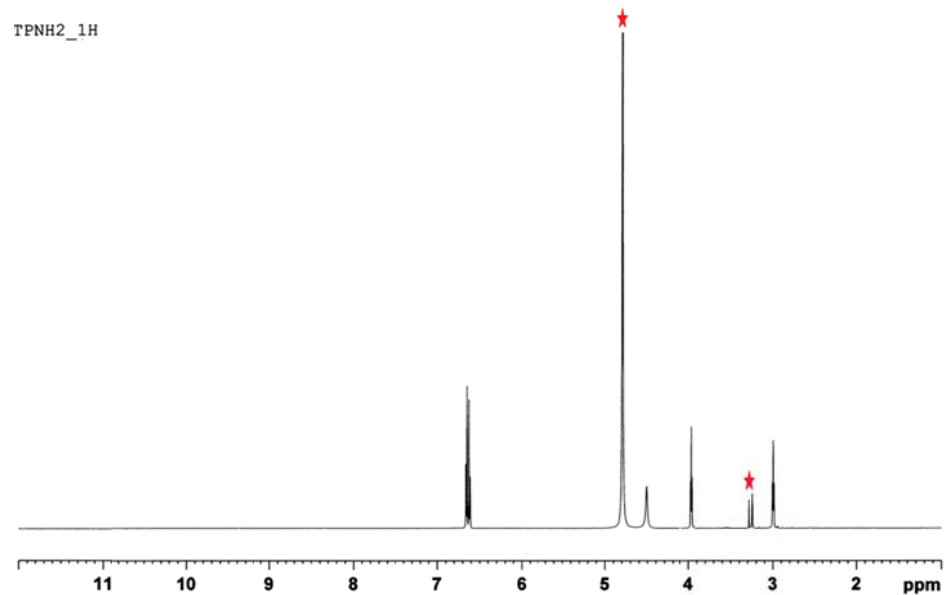


Fig. S1 ¹H-NMR spectrum of receptor **L** in CD₃OD at 298 K. Indicated peaks represent the solvent.

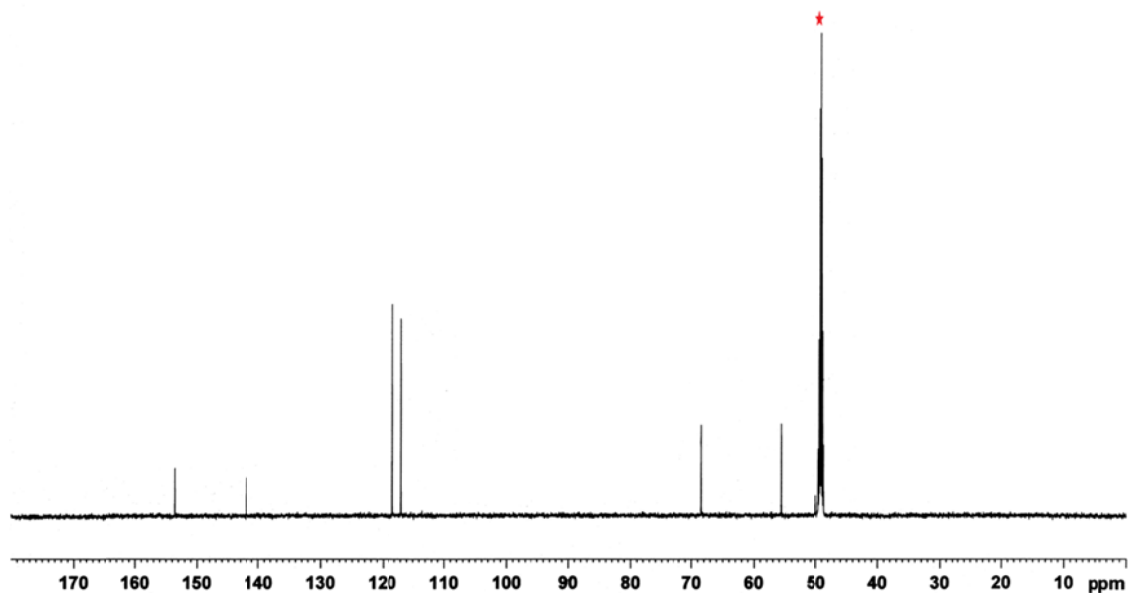


Fig. S2 ¹³C-NMR spectrum of receptor **L** in CD₃OD at 298 K. Indicated peak represent the solvent.

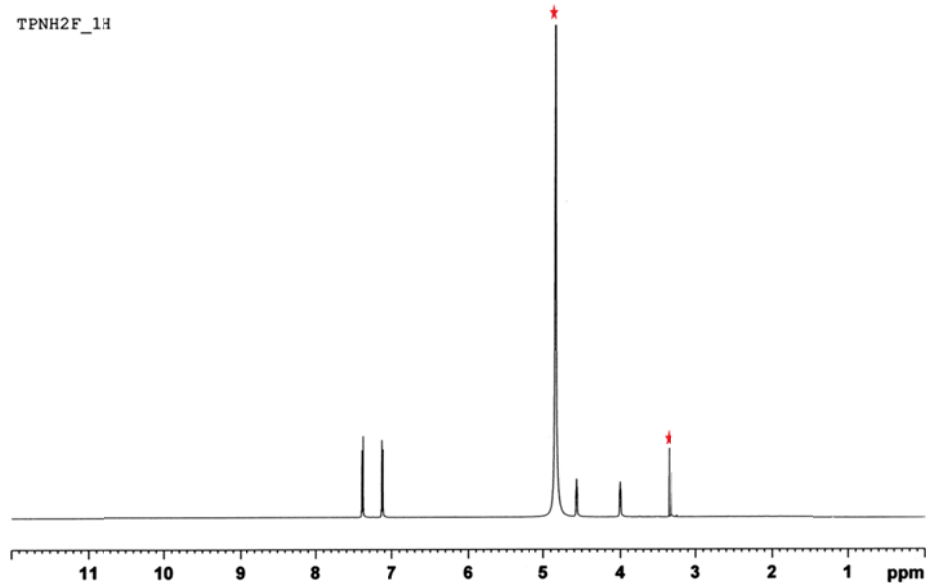


Fig. S3 ¹H-NMR spectrum of complex [LH₄·4F·5H₂O](**1**) in CD₃OD:D₂O (1:2) at 298 K. Indicated peaks represent the solvent.

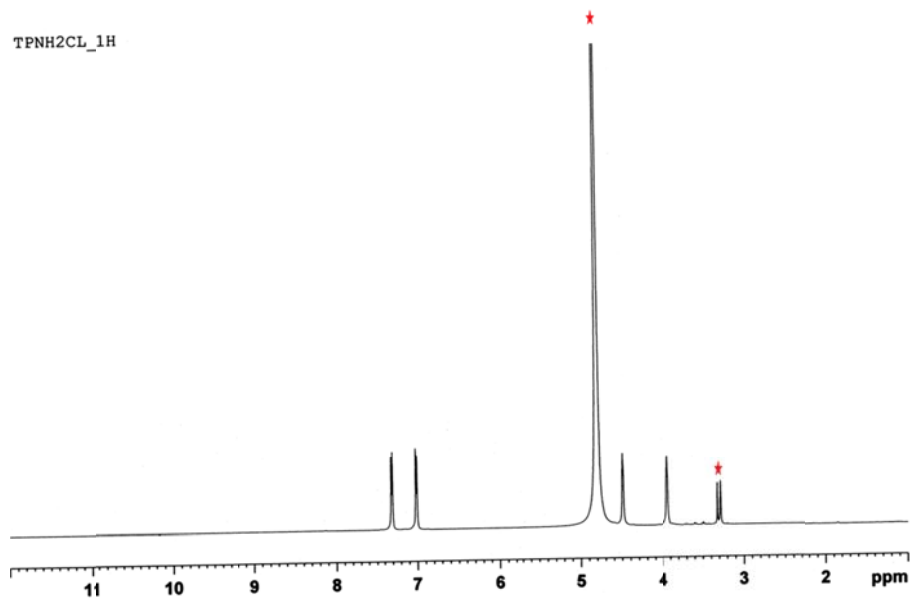


Fig. S4 ¹H-NMR spectrum of complex [2LH₄·8Cl·5H₂O](2) in CD₃OD:D₂O (1:2) at 298 K.

Indicated peaks represent the solvent.

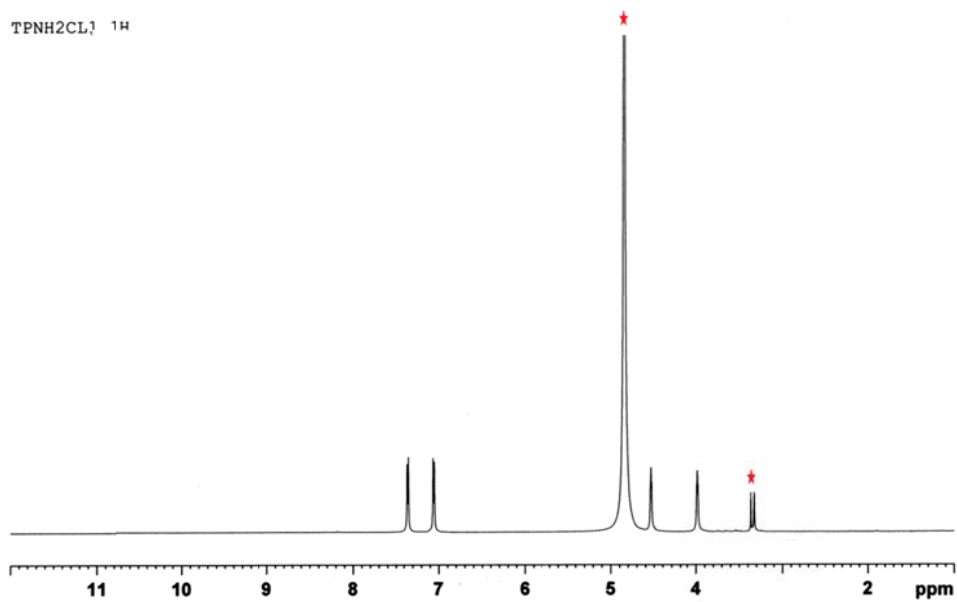


Fig. S5 ¹H-NMR spectrum of complex [LH₄·4Cl](3) in CD₃OD:D₂O (1:2) at 298 K. Indicated peaks represent the solvent.

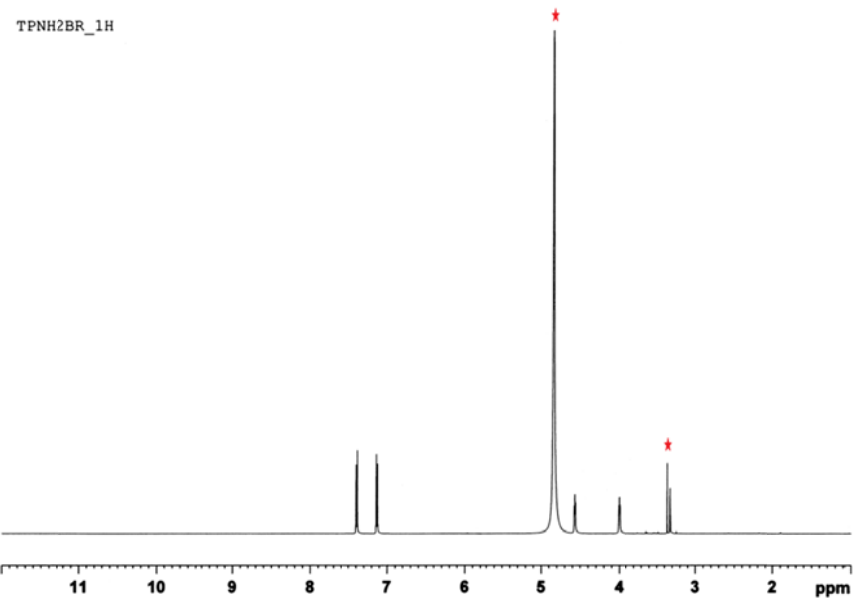


Fig. S6 ¹H-NMR spectrum of complex $[\text{LH}_4 \cdot 4\text{Br} \cdot 5\text{H}_2\text{O}](4)$ in $\text{CD}_3\text{OD:D}_2\text{O}$ (1:2) at 298 K.

Indicated peaks represent the solvent.

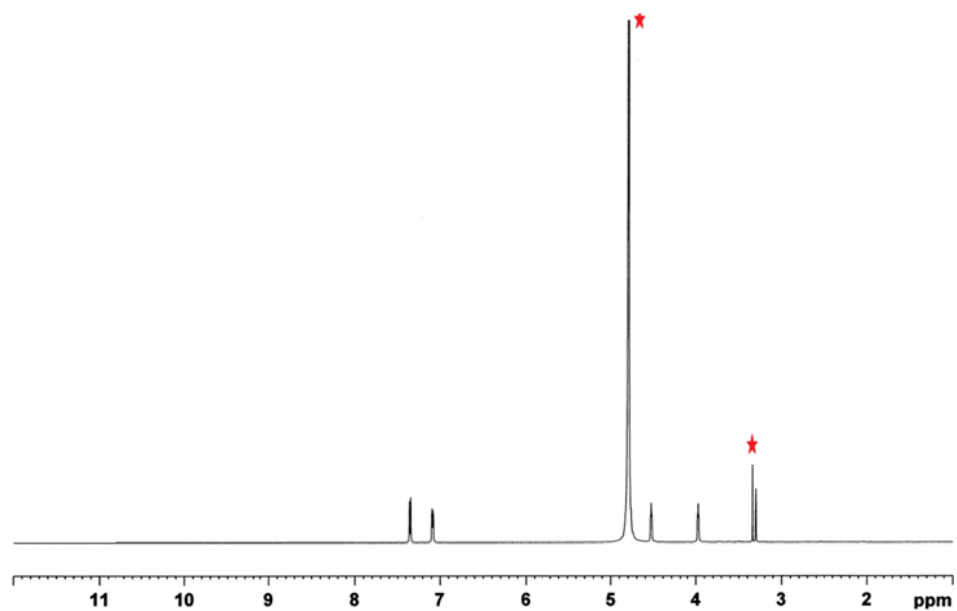


Fig. S7 ¹H-NMR spectrum of complex $[4\text{LH}_4 \cdot 16\text{I}^7 \cdot \text{H}_2\text{O}](5)$ in $\text{CD}_3\text{OD:D}_2\text{O}$ (1:2) at 298 K.

Indicated peaks represent the solvent.

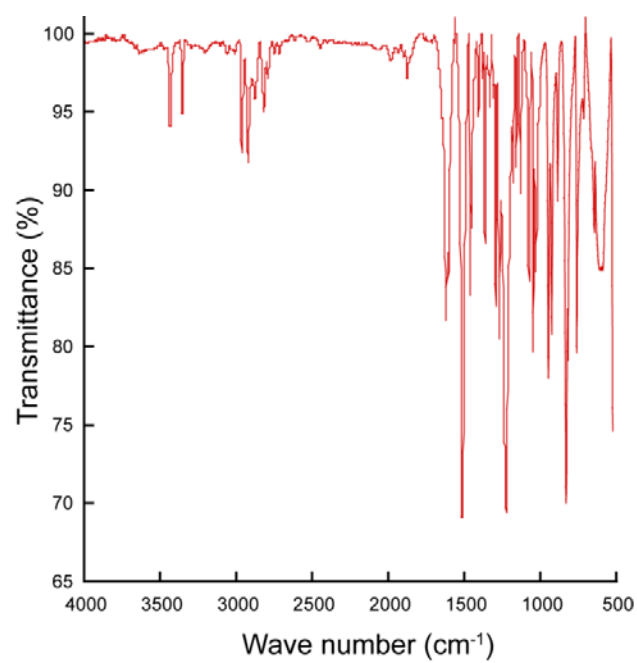


Fig. S8 FT-IR spectrum of free receptor **L**.

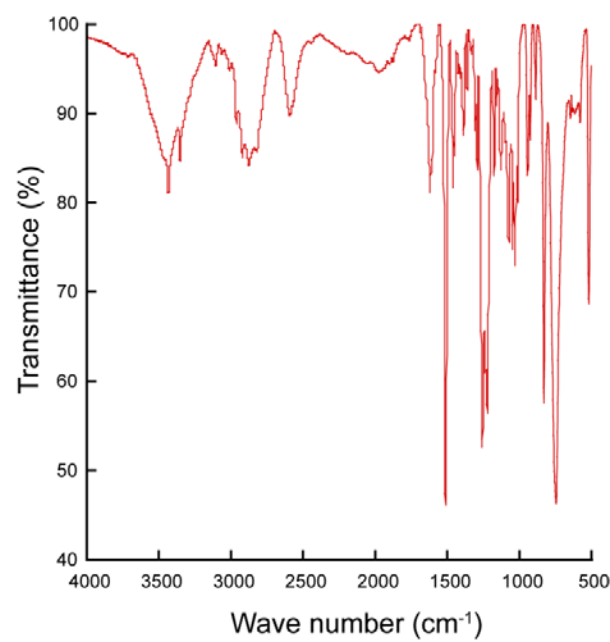


Fig. S9 FT-IR spectrum of complex $[\text{LH}_4 \cdot 4\text{F} \cdot 5\text{H}_2\text{O}](1)$.

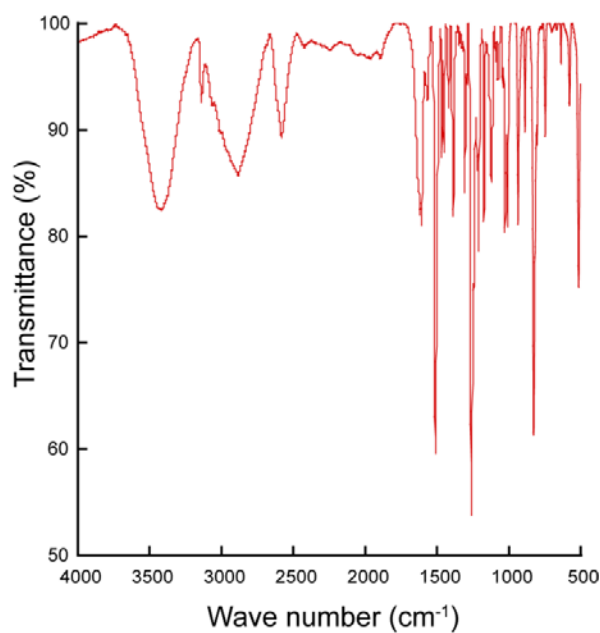


Fig. S10 FT-IR spectrum of complex $[2\text{LH}_4 \cdot 8\text{Cl} \cdot 5\text{H}_2\text{O}](2)$.

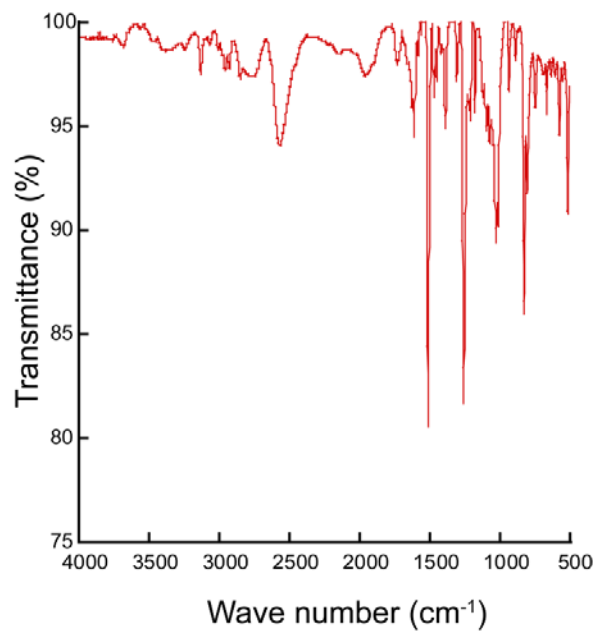


Fig. S11 FT-IR spectrum of complex $[\text{LH}_4 \cdot 4\text{Cl}](3)$.

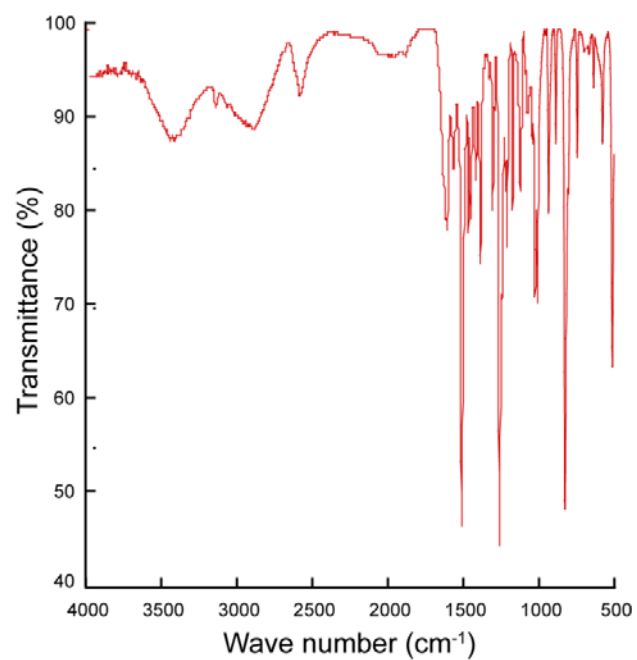


Fig. S12 FT-IR spectrum of complex $[\text{LH}_4 \cdot 4\text{Br} \cdot 5\text{H}_2\text{O}](4)$.

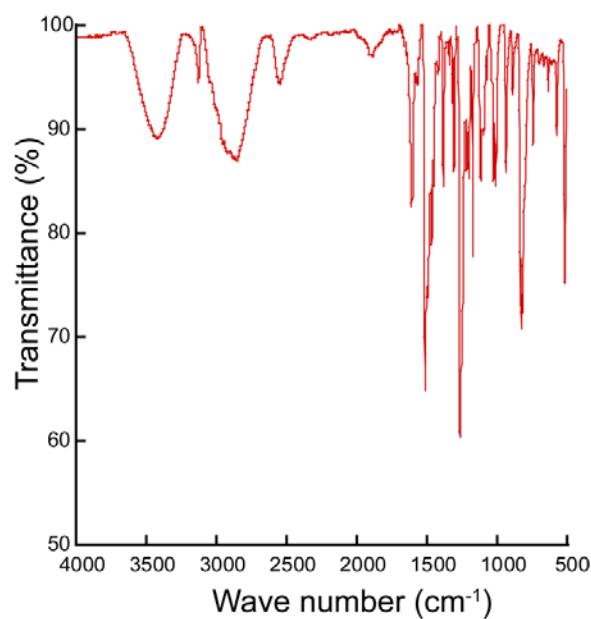


Fig. S13 FT-IR spectrum of complex $[4\text{LH}_4 \cdot 16\text{I} \cdot 7\text{H}_2\text{O}](5)$.

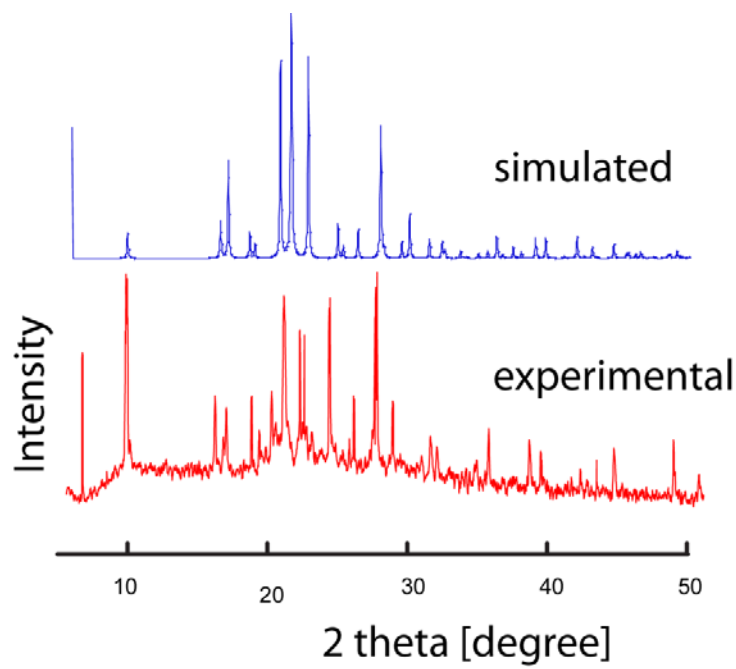


Fig. S14 Powder X-ray diffraction: simulated pattern from the single crystal X-ray of free receptor **L** (blue), experimental pattern from the crystalline solid of free receptor **L** (red).

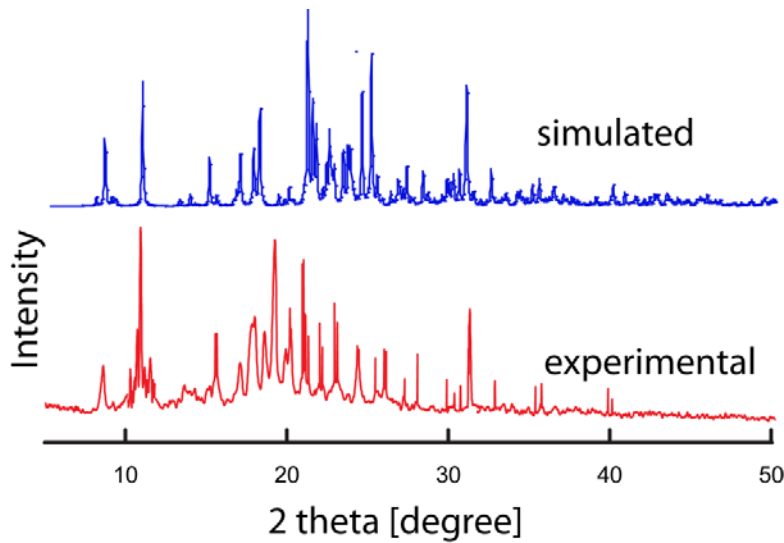


Fig. S15 Powder X-ray diffraction: simulated pattern from the single crystal X-ray of complex $[\text{LH}_4 \cdot 4\text{F} \cdot 5\text{H}_2\text{O}](\mathbf{1})$ (blue), experimental pattern from the crystalline solid of complex $[\text{LH}_4 \cdot 4\text{F} \cdot 5\text{H}_2\text{O}](\mathbf{1})$ (red).

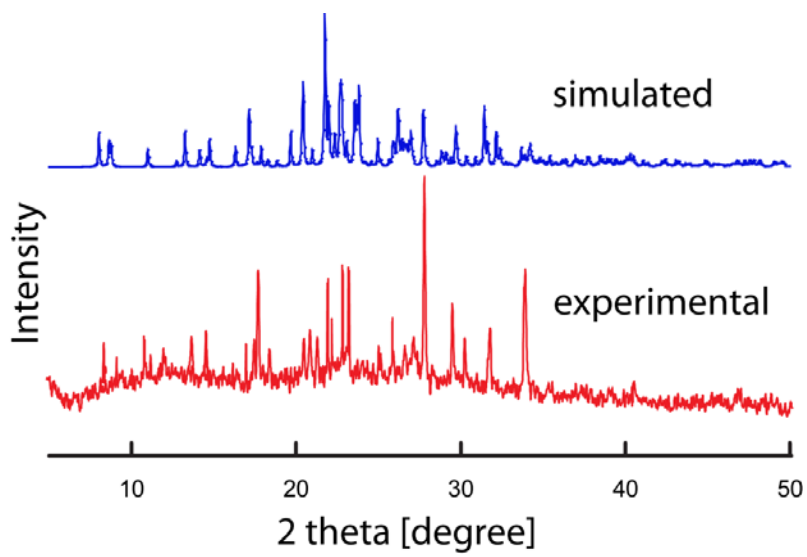


Fig. S16 Powder X-ray diffraction: simulated pattern from the single crystal X-ray of complex $[2\text{LH}_4 \cdot 8\text{Cl} \cdot 5\text{H}_2\text{O}](2)$ (blue), experimental pattern from the crystalline solid of complex $[2\text{LH}_4 \cdot 8\text{Cl} \cdot 5\text{H}_2\text{O}](2)$ (red).

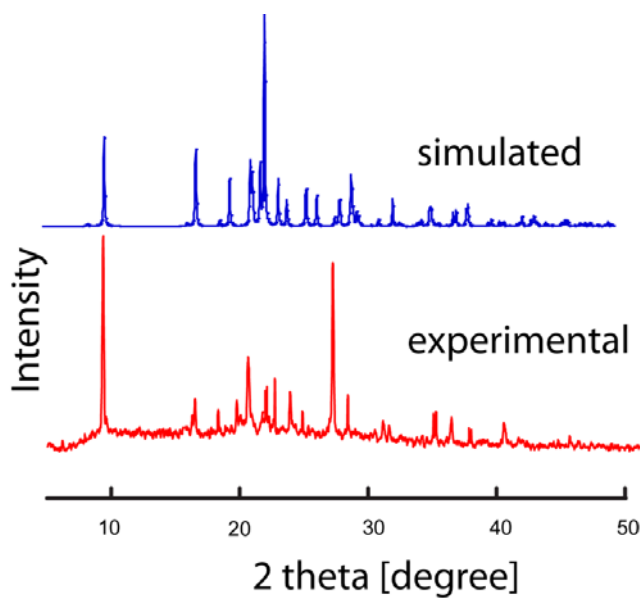


Fig. S17 Powder X-ray diffraction: simulated pattern from the single crystal X-ray of complex $[\text{LH}_4 \cdot 4\text{Cl}](3)$ (blue), experimental pattern from the crystalline solid of complex $[\text{LH}_4 \cdot 4\text{Cl}](3)$ (red).

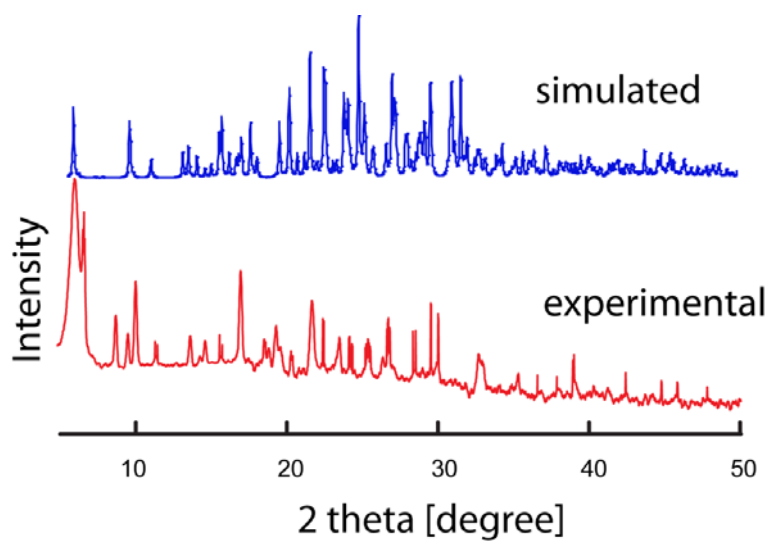


Fig. S18 Powder X-ray diffraction: simulated pattern from the single crystal X-ray of complex $[\text{LH}_4 \cdot 4\text{Br} \cdot 5\text{H}_2\text{O}](\mathbf{4})$ (blue), experimental pattern from the crystalline solid of complex $[\text{LH}_4 \cdot 4\text{Br} \cdot 5\text{H}_2\text{O}](\mathbf{4})$ (red).

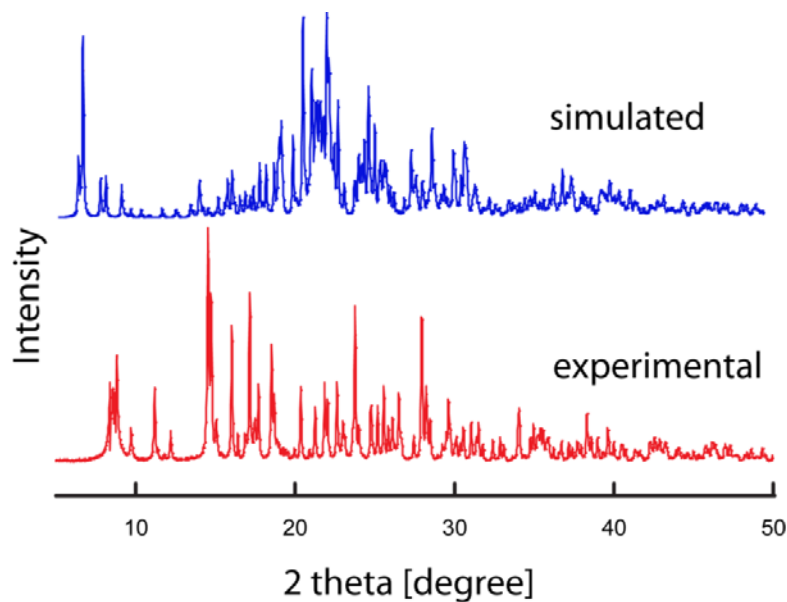


Fig. S19 Powder X-ray diffraction: simulated pattern from the single crystal X-ray of complex $[4\text{LH}_4 \cdot 16\text{I} \cdot 7\text{H}_2\text{O}](\mathbf{5})$ (blue), experimental pattern from the crystalline solid of complex $[4\text{LH}_4 \cdot 16\text{I} \cdot 7\text{H}_2\text{O}](\mathbf{5})$ (red).

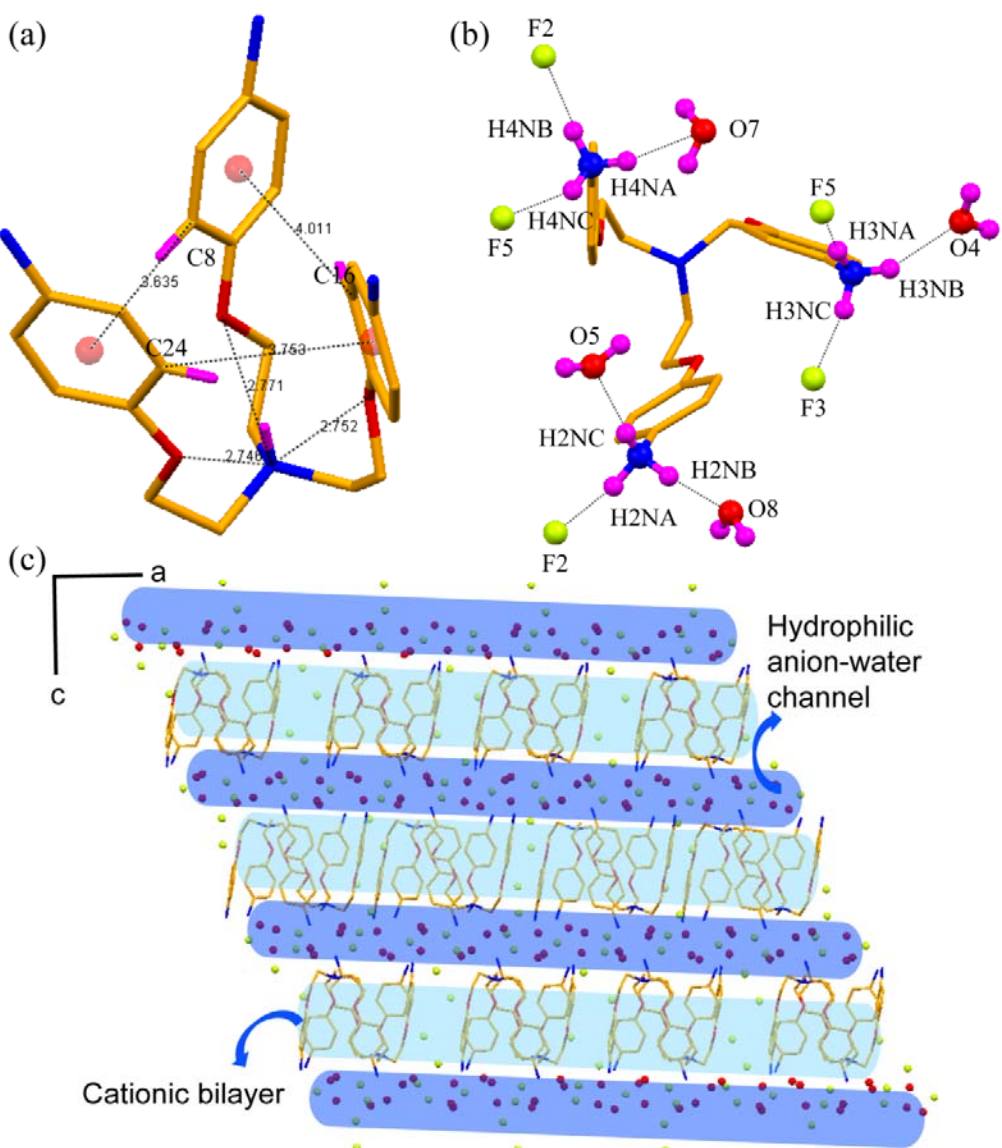


Fig. S20 (a) Showing N—H···O and C—H···π interactions that stabilized the bowl shaped conformation of the tripodal receptor in complex 1. (b) Depicting H-bonding interactions of $[\text{NH}_3^+]$ groups with fluoride ions and water molecules. (c) Crystal packing as viewed down along *b*-axis showing the cationic bilayer assembly formation of ligand moieties diagonally with the fluoride-water entrapped between the adjacent ligand arrays forming hydrophilic anion-water channel.

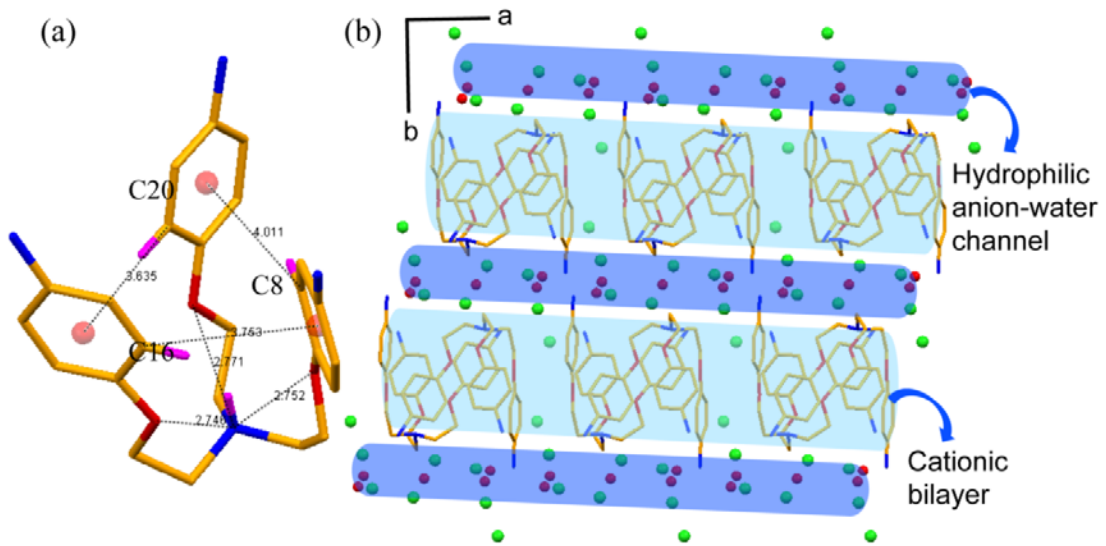


Fig. S21 (a) Showing N—H \cdots O and C—H \cdots π interactions that stabilized the bowl shaped conformation of the tripodal receptor in complex **2**. (b) Crystal packing as viewed down along *b*-axis showing the cationic bilayer assembly formation of ligand moieties diagonally with the chloride-water entrapped between the adjacent ligand arrays forming hydrophilic anion-water channel in complex **2**.

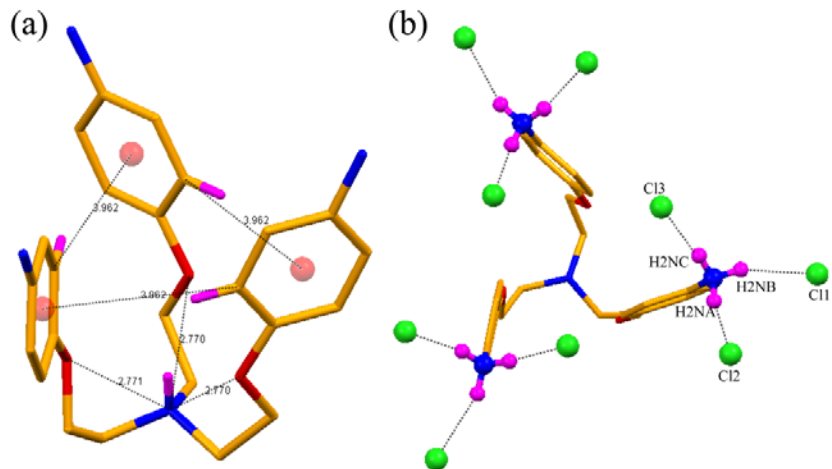


Fig. S22 (a) Showing N—H \cdots O and C—H \cdots π interactions that stabilized the bowl shaped conformation of the tripodal receptor in complex **3**. (b) Depicting H-bonding interactions of $[\text{NH}_3^+]$ groups with chloride ions.

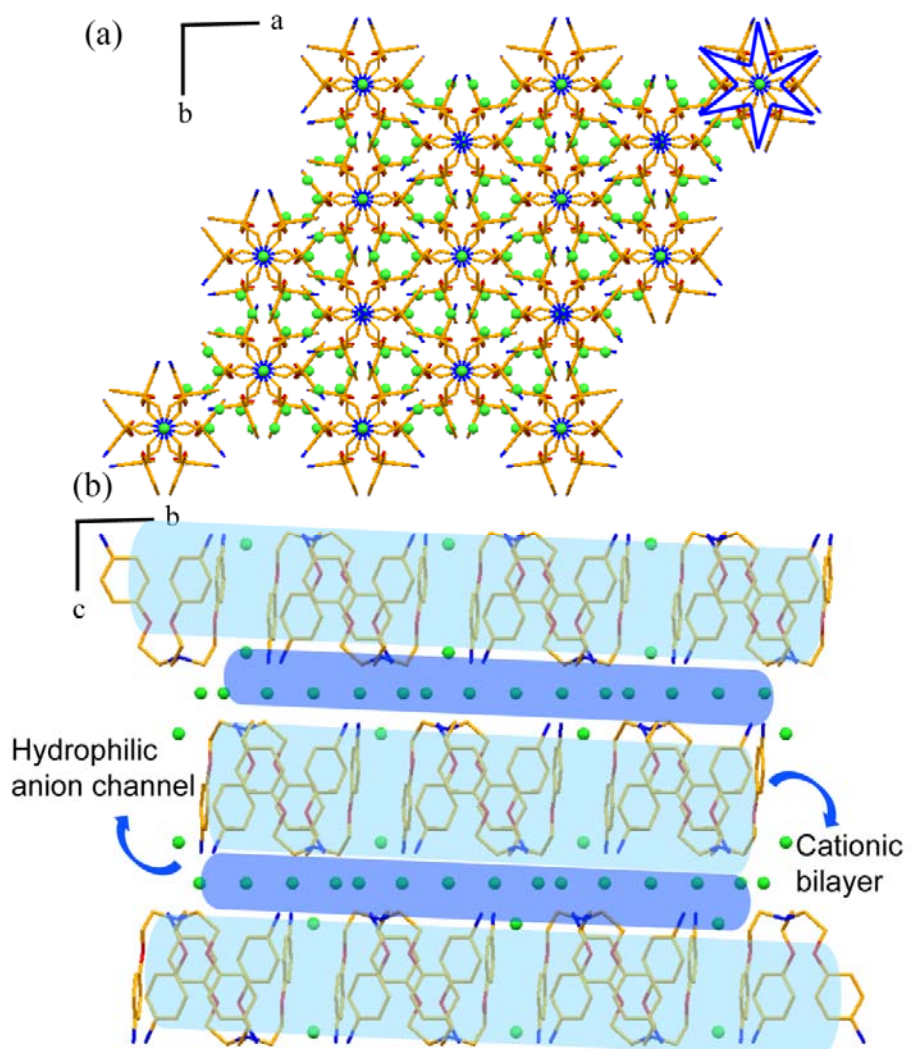


Fig. S23 (a) Crystal packing along c -axis shows star like arrangement of tripodal receptor in capsular complex **3**. (b) Crystal packing viewed along a -axis shows chloride ion channel between cationic bilayer of tripodal receptor.

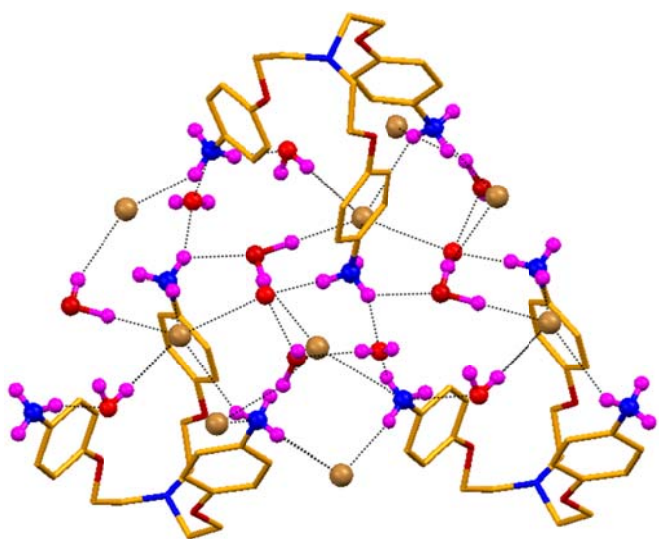


Fig. S24 Non-capsular assembly of complex **4** mediated by several bromide-water cluster H-bonding interactions.

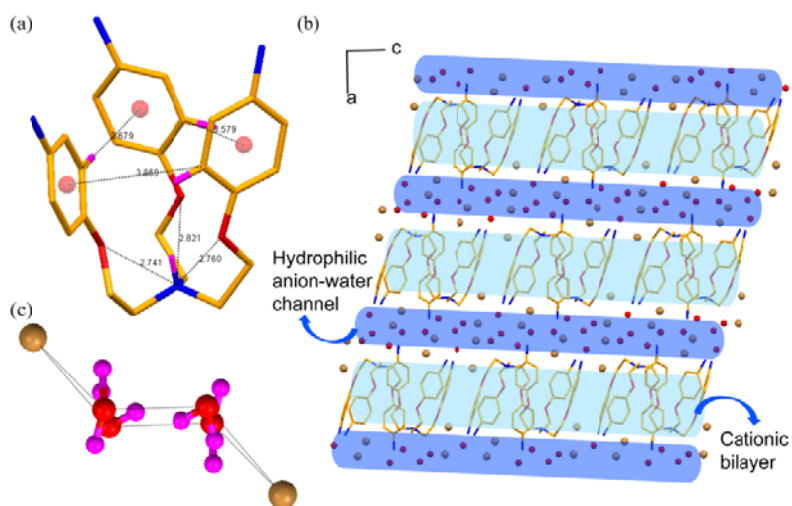


Fig. S25 (a) Showing N—H \cdots O and C—H \cdots π interactions that stabilized the bowl shaped conformation of the tripodal receptor in complex **4**. (b) Crystal packing as viewed down along *b*-axis showing the cationic bilayer assembly formation of ligand moieties diagonally with hydrophilic bromide-water channel entrapped between the adjacent ligand arrays in complex **4**. (c) Chair conformation of hexameric bromide-water cluster.

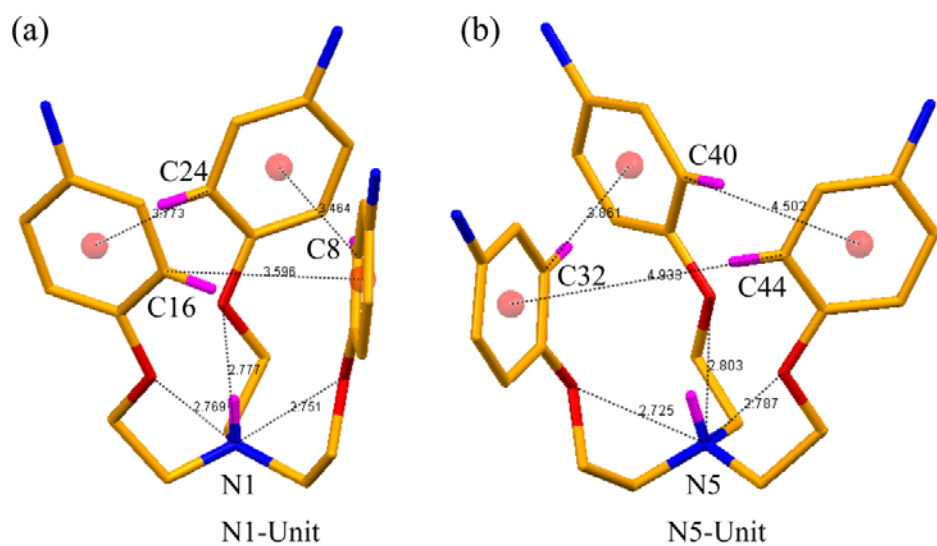


Fig. S26 (a) and (b) Showing N—H···O and C—H···π interactions that stabilized the bowl shaped conformation in N1 and N5 unit in complex **5**.

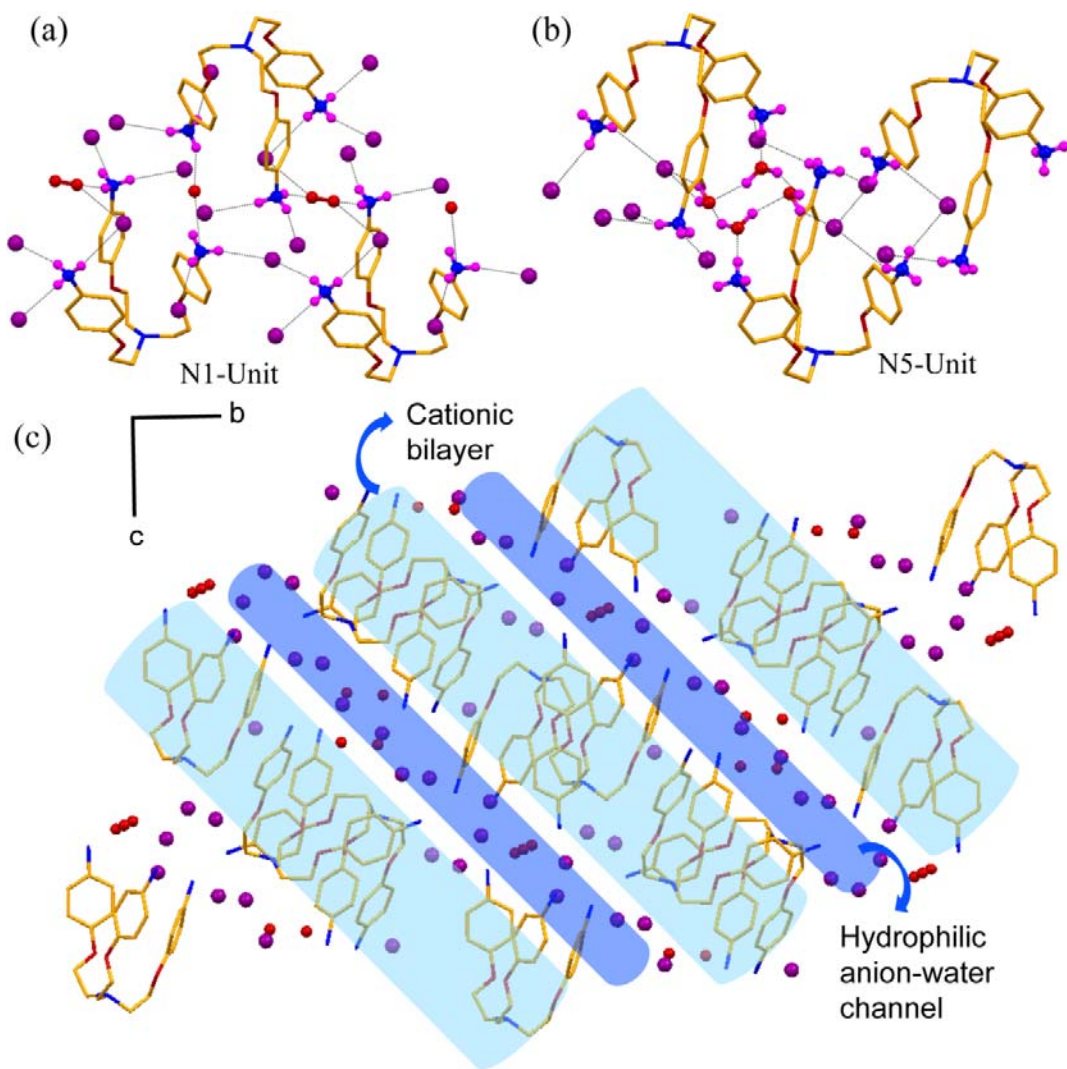


Fig. S27 (a) and (b) Non-capsular assembly of two symmetry independent N1 and N5 unit mediated by several iodide-water H-bonding interactions in complex **5**. (c) Crystal packing as viewed down along *a*-axis showing the cationic bilayer assembly formation of ligand moieties diagonally with hydrophilic iodide-water channel entrapped between the adjacent ligand arrays in complex **5**.

Table S1 Relevant H-boning parameters details for compounds **1-6**.

D—H···A [L]	d(D···A) Å	d(H···A) Å	\angle (D—H—A)/°
C5—H···O1	3.536(1)	2.683(1)	152.7(9)
C8—H···N2	3.593(3)	2.733(2)	154.2(1)
N2—H···C2	3.611(3)	3.0451(1)	125.4(2)
[LH₄·4F·5H₂O](1)			
N2—H2NA···F2	2.679(5)	1.720(3)	170.0(2)
N2—H2NB···O8w	2.606(6)	1.740(6)	162.0(5)
N2—H2NC···O5w	2.739(6)	1.960(6)	165.0(6)
N3—H3NA···F5	2.604(3)	1.727(2)	168.1(2)
N3—H3NB···O4w	2.828(4)	2.00(5)	153.4(2)
N3—H3NC···F3	2.691(3)	1.811(2)	168.6(2)
N4—H4NA···O7w	2.767(5)	1.922(3)	157.6(3)
N4—H4NB···F2	2.766(5)	1.892(2)	167.1(3)
N4—H4NC···F5	2.683(4)	1.888(2)	147.7(3)
O4w—H4A···F3	2.767(4)	1.933(3)	166.6(20)
O4w—H4B···F2	2.739(3)	1.941(2)	156.1(2)
O5w—H5B···F1	2.819(7)	2.100(1)	143.0(12)
O5w—H5A···F3	2.280(5)	1.465(2)	159.6(4)
O6w—H6A···F5	2.370(4)	1.540(3)	164.0(4)
O8w—H8A···F2	3.172(5)	2.487(3)	138.4(2)
C5—H5···F4	3.454(6)	2.528(4)	173.8(2)
C13—H13···F4	3.145(5)	2.320(4)	147.6(2)
C20—H20···F4	3.273(5)	2.459(4)	146.3(2)
C1—H1A···O4W	3.400(4)	2.618(2)	137.9(2)
C17—H17B···O6W	3.368(4)	2.493(3)	149.7(2)
[2LH₄·8Cl₄·5H₂O](2)			
N2—H2NA···Cl1	3.286(4)	2.305(7)	165.0(2)
N2—H2NB···Cl3	3.174(3)	2.392(1)	151.7(2)
N2—H2NC···Cl2	3.072(4)	2.187(1)	172.4(2)
N3—H3NA···Cl4	3.160(3)	2.450(4)	152.0(4)
N3—H3NB···Cl3	3.225(3)	2.430(4)	148.0(5)
N3—H3NA···Cl1	3.221(4)	2.600(3)	165.0(4)
N4—H4NA···O5w	2.743(6)	1.863(5)	149.0(4)
N3—H3NA···Cl1	3.244(5)	2.536(3)	169.7(2)
N4—H4NB···Cl4	3.087(2)	2.220(6)	164.5(2)
N4—H4NC···Cl3	3.218(3)	2.399(1)	153.0(2)
C4—H4···Cl1	3.574(3)	2.893(7)	131.2(2)
C12—H12···Cl1	3.523(4)	2.819(1)	133.4(2)
C23—H23···Cl1	3.732(3)	2.940(1)	144.0(2)
O5w—H5A···Cl1	3.184(3)	2.380(5)	172.0(6)
C1—H1B···Cl2	3.515(3)	2.747(9)	136.4(2)

C10—H10B···Cl2	3.751(3)	2.887(1)	149.0(2)
O4w—H4A···Cl2	3.187(3)	2.354(1)	144.6(2)
C17—H17···Cl3	3.554(4)	2.814(1)	133.6(2)
O4w—H4B···Cl3	3.203(4)	2.403(1)	157.0(2)
C2—H2A···Cl4	3.673(3)	2.867(7)	141.0(2)
C9—H9A···Cl4	3.618(3)	2.648(7)	139.2(2)
O5w—H5B···Cl4	3.141(5)	2.300(1)	147.0(7)
[LH₄·4Cl](3)			
N2—H2NB···Cl1	3.041(3)	2.165(6)	163.8(2)
N2—H2NA···Cl2	3.184(2)	2.334(2)	120.6(2)
N2—H2NC···Cl1	3.038(3)	2.152(1)	135.0(3)
C1—H1A···Cl1	3.543(3)	2.855(6)	128.5(2)
C1—H1B···Cl1	3.724(2)	2.899(3)	143.4(2)
[LH₄·4Br·5H₂O](4)			
N2—H2NA···Br1	3.225(5)	2.359(7)	164.3(3)
N2—H2NB···Br3	3.603(4)	3.043(6)	122.7(3)
N2—H2NC···Br4	3.321(5)	2.453(6)	165.4(3)
N3—H3NA···Br3	3.415(5)	2.545(8)	165.5(30)
N3—H3NB···O6w	2.782(7)	1.911(5)	165.6(4)
N3—H3NC···O5w	2.809(6)	1.996(5)	151.4(4)
N4—H4NA···O4w	2.771(8)	1.911(6)	161.9(4)
N4—H4NB···Br4	3.388(5)	2.501(7)	173.1(3)
N4—H4NC···Br1	3.344(5)	2.554(6)	148.2(3)
C9—H9B···Br1	3.621(6)	2.821(7)	140.3(3)
O8w—H8OB···Br1	3.475(7)	2.660(9)	146.0(7)
C1—H1B···Br2	3.832(5)	2.901(6)	161.1(3)
O4w—H4OA···Br2	3.263(7)	2.650(8)	125.0(6)
O5w—H5OB···Br2	3.358(6)	2.600(1)	142.0(9)
O7w—H7OA···Br2	3.264(7)	2.400(1)	126.0(8)
O4w—H4OB···Br3	3.319(6)	2.500(7)	176.0(8)
O8w—H4OA···Br3	3.528(7)	2.300(2)	175.0(11)
C4—H4···Br4	3.717(5)	2.889(6)	149.0(3)
O7w—H7OB···Br4	3.258(8)	2.360(4)	157.0(3)
[4LH₄·16I·7H₂O] (5)			
N2—H2NA···I5	3.461(9)	2.629(6)	156.3(6)
N2—H2NB···I6	3.551(9)	2.687(6)	158.3(8)
N2—H2NC···O9w	2.920(3)	2.070(2)	164.2(6)
N3—H3NA···I2	3.565(9)	2.693(7)	166.8(6)
N3—H3NB···O8w	2.941(8)	2.119(1)	153.2(6)
N3—H3NC···O5w	3.546(8)	2.717(8)	155.3(6)
N4—H4NA···I2	3.547(8)	2.686(7)	163.1(5)
N4—H4NB···I1	3.696(7)	2.878(8)	153.4(5)
N4—H4NC···I3	3.480(8)	2.639(8)	157.8(5)
N6—H6NA···I7	3.550(1)	2.671(1)	171.2(9)

N6—H6NB···I8	3.530(1)	2.778(9)	143.2(9)
N6—H6NC···O7w	2.780(3)	1.910(3)	163.0(1)
N7—H7NA···I7	3.650(1)	2.967(1)	134.5(9)
N7—H7NB···I8	3.600(2)	2.744(2)	160.8(9)
N8—H8NA···I3	3.492(9)	2.870(8)	128.3(6)
N8—H8NA···I5	3.764(9)	3.151(6)	127.9(6)
N8—H8NB···I6	3.518(8)	2.658(6)	162.7(6)
N8—H8NC···I6	3.680(1)	2.835(9)	158.2(6)
O8···I6	3.711(7)	---	---
I1···O9	3.320(2)	---	---
C39—H39···I3	3.820(1)	3.113(8)	134.2(8)
C41—H41···I4	3.850(1)	2.927(1)	160.2(6)
O10—H10C···I4	3.630(3)	2.800(2)	148.0(17)
C17—H17···I5	3.930(1)	3.150(6)	144.6(7)
C34—H34···I5	3.850(1)	3.019(6)	139.0(6)
C9—H9B···I6	3.863(9)	3.119(7)	134.7(6)
C29—H29···I7	3.800(1)	2.962(1)	150.1(8)
C25—H25···I8	3.890(1)	3.060(9)	145.0(7)
O10···I8	3.730(3)	---	---